Journal of Power Sources 255 (2014) 125–129

Contents lists available at ScienceDirect

Journal of Power Sources

journal homepage: www.elsevier.com/locate/jpowsour

Short communication

High-performance anode based on porous Co_3O_4 nanodiscs

Anqiang Pan [a,b,*], Yaping Wang [a], Wu Xu [b], Zhiwei Nie [a], Shuquan Liang [a,**], Zimin Nie [b], Chongmin Wang [b], Guozhong Cao [c], Ji-Guang Zhang [b,**]

[a] School of Materials Science and Engineering, Central South University, Changsha 410083, Hunan, China
[b] Pacific Northwest National Laboratory, Richland, WA 99354, USA
[c] Department of Materials Science & Engineering, University of Washington, WA 98195, USA

HIGHLIGHTS

- Porous Co_3O_4 hexagonal nanodiscs were prepared by a template-free hydrothermal method.
- The Co_3O_4 hexagonal nanodiscs are about 20 nm in thickness and the pore diameters range from several nm to 30 nm.
- The Co_3O_4 hexagonal nanodiscs exhibit excellent electrochemical performance as anode materials for lithium ion batteries.

ARTICLE INFO

Article history:
Received 29 September 2013
Received in revised form
27 December 2013
Accepted 31 December 2013
Available online 8 January 2014

Keywords:
Cobalt oxide
Hydrothermal
Lithium-ion batteries
Hexagonal nanodiscs
Anode

ABSTRACT

In this article, two-dimensional, Co_3O_4 hexagonal nanodiscs are prepared using a hydrothermal method without surfactants. X-ray diffraction (XRD), scanning electron microscopy (SEM), and transmission electron microscopy (TEM) have been employed to characterize the structural properties. As revealed by the SEM and TEM experiments, the thickness of our as-fabricated Co_3O_4 hexagonal nanodiscs is about 20 nm, and the pore diameters range from several nanometers to 30 nm. As an anode for lithium-ion batteries, porous Co_3O_4 nanodiscs exhibit an average discharge voltage of ~1 V (vs. Li/Li^+) and a high specific charge capacity of 1161 mAh g^{-1} after 100 cycles. They also demonstrate excellent rate performance and high Columbic efficiency at various rates. These results indicate that porous Co_3O_4 nanodiscs are good candidates as anode materials for lithium-ion batteries.

1. Introduction

High energy storage systems are needed to reduce our reliance on fossil fuels and minimize environmental pollution associated with the use of fossil fuels [1]. Because of the high energy density, long cycle life, and flexible design, lithium-ion batteries have become the dominant power sources for high-end consumer electronic devices such as cell phones, laptop computers, and, more recently, hybrid and electrical vehicles. However, the need to provide higher energy and power levels becomes more acute with rapidly increasing demand for applications such as long-range electrical vehicles. The specific capacity achievable with conventional graphite anodes used in commercial lithium-ion batteries is limited (<370 mAh g^{-1}). Various materials—for example, graphitic/non-graphitic carbons [2], silicon- or tin-based lithium alloys [3–6], transition-metal oxides [7–10], and nitrides [11]—have been studied as alternative anode materials for lithium-ion batteries because they can provide higher capacities. As an important p-type semiconductor, cobalt oxide has gained extensive interest as an anode material for lithium-ion batteries because of its high theoretical capacity (890 mAh g^{-1}) [12,13]. However, the electrochemical performance, such as specific capacity and cycling stability, degrades rapidly because of the large volume expansions/contractions associated with the lithium-ion injection and extraction processes [14–16] and side reactions, such as the reductive decomposition of the electrolyte [17]. Nanomaterials are favored because of their novel properties, such as larger surface areas, shorter lithium-ion-diffusion and electron-transportation distances, and better ability to accommodate volume changes that occur during charge/discharge cycles [15]. Therefore, enabling long-term cycle stability of a Co_3O_4-based anode material is still a significant challenge. Up till to now, Co_3O_4 nanomaterials of

* Corresponding author. School of Materials Science and Engineering, Central South University, Changsha 410083, Hunan, China.
** Corresponding authors.
E-mail addresses: pananqiang@gmail.com (A. Pan), lsq@mail.csu.edu.cn (S. Liang), jiguang.zhang@pnl.gov (J.-G. Zhang).

0378-7753/$ – see front matter © 2014 Elsevier B.V. All rights reserved.
http://dx.doi.org/10.1016/j.jpowsour.2013.12.131

different morphologies, such as zero-dimensional nanoparticles [18]; one dimensional nanowires [19–21]; nanorods [22,23]; nanotubes [23,24]; nanoneedles [25], two-dimensional nanodiscs, nanosheets, nanomesh, or nanoplatelets [26–29]; three-dimensional nanocubes; and hierarchical nanoflowers [17], have been fabricated. It has been found that capacity, rate capability, and capacity retention are strongly dependent on the morphologies of the Co_3O_4 nanomaterials. Nanomaterials with porous structures have attracted much attention because they possess higher surface areas and available pathways for rapid penetration of electrolytes [24,25,29]. Wang et al. [29] reported successful synthesis of a two-dimensional functional Co_3O_4 nanomesh with the highest documented surface area (382 $m^2\ g^{-1}$) and an extremely high specific capacity ($\sim$1800 mAh g^{-1}). However, the capacity quickly fades to $\sim$800 mAh g^{-1} at 50 cycles, and the Columbic efficiency is relative low (90%). This performance degradation is probably associated with electrolyte decomposition and side reactions caused by the high surface area. Therefore, better cycling stability would be expected for materials with lower surface areas. Also, the purity of the active materials is another key factor to obtaining stable performance. To synthesize a nanoparticle with a particular shape, a surfactant typically is employed as a soft template during synthesis [17,30,31]. However, the surfactant must be removed, and incomplete removal may result in inferior performance of the material because of the impurity and low crystallinity. Introduction of the surfactant removal process makes fabrication more complicated and expensive.

In this article, we report a facile approach for synthesizing porous Co_3O_4 hexagonal nanodiscs without using a surfactant. Our as-prepared nanomaterials have low surface areas and a high purity, which reduces side reactions, such as electrolyte decomposition. The structure of the Co_3O_4 nanodiscs is characterized and excellent electrochemical performances of the Co_3O_4 nanodiscs after activation are reported.

2. Experimental section

$Co(OH)_2$ nanorods as the precursor for Co_3O_4 were prepared using a hydrothermal process. $Co(NO_3)_2{\cdot}6H_2O$ (1.26 g) was dissolved in 20 mL distilled water, and then, a 20-mL NaOH (0.432 g) aqueous solution was added drop by drop. The mixture was stirred 30 min to form a brown color before it was transferred to a 40-mL, teflon-lined, stainless-steel autoclave. The reaction was maintained at 140 °C for 12 h. After cooling to room temperature, $Co(OH)_2$ that had precipitated from the solution was washed with distilled water and collected by vacuum filtration several times. The resulting film was dried under vacuum at 80 °C overnight and then baked in air at 450 °C for 2 h.

The crystalline structure of the as-prepared $Co(OH)_2$ precursor and its annealed products in air were determined by XRD analysis using a Scintag XDS2000 θ–θ powder diffractometer equipped with a germanium (lithium) solid-state detector and a copper Kα sealed tube (λ = 1.54178 Å). The samples were scanned in the range between 10° and 70° (2θ), with a step size of 0.02° and an exposure time of 10 s. SEM analysis was carried out on an FEI Helios 600 Nanolab FIB-SEM, 3 KV to characterize the particle morphology, while TEM analysis was carried out on a Jeol JEM 2010 microscope fitted with a LaB_6 filament and at an acceleration voltage of 200 kV. Nitrogen adsorption–desorption measurements were conducted at 77 K (NOVA 4200e, Quantachrome Instruments). Co_3O_4 was degassed at 200 °C for 18 h before adsorption and desorption measurements. The sample weight for nitrogen adsorption–desorption analysis is about 200 mg.

To prepare the electrode, Co_3O_4 was mixed with Super P carbon and poly(vinylidene fluoride) (PVDF) binder (at a weight ratio of 8:1:1) in *N*-methyl-2-pyrrolidone to make a slurry that was cast onto copper foil and dried in a vacuum oven at 100 °C overnight.

Electrodes were tested in coin cells (2325 coin cell, National Research Council, Canada) assembled in a glove box (MBraun, Inc.) filled with ultra-high-purity argon. The cells used polypropylene membrane (Celgard 3501) as the separator, lithium metal as the anode, and 1-M $LiPF_6$ in ethyl carbonate/dimethyl carbonate (1:1 v/v) as the electrolyte. The electrochemical performances of the electrodes were evaluated in an Arbin Battery Tester BT-2000 (Arbin Instruments) at room temperature. The cobalt oxides cells were tested in a voltage range of 0.01–3 V vs. Li/Li^+ at various charging/discharging rates. The capacity reported in this work is based on the total weight of Co_3O_4 and conductive carbon. The loading of the cathode materials is 1–2 mg cm^{-2} with the thickness of 5 μm.

3. Results and discussions

Fig. 1 shows the XRD patterns for the hydrothermally prepared precursor and its annealed products in air at 450 °C for 2 h. Most of the precursor's peaks, assigned to $Co(OH)_2$ (JCPDS card No. 45-0031, space group $P-3m1$), have been indexed. However, a small amount of Co_3O_4 phase also is detected as indicated by the arrows, suggesting that the Co^{2+} has been partially oxidized to Co^{3+} in the precursors. The XRD pattern for the annealed sample aligns well with the standard XRD pattern of Co_3O_4 (JCPDS card No. 43-1003, space group $Fd3m$), and no other phase is detected. This result indicates full oxidation of Co^{2+} and the high purity level of the Co_3O_4 nanodiscs.

Fig. 2 shows the morphologies and structure information of as-prepared Co_3O_4 nanodiscs. As shown in Fig. 2a, most of the particles are hexagonal in shape with some small particles attached on the surface. Large spaces between hexagonal nanodiscs also are observed clearly. Fig. 2b shows the TEM image of nanodiscs. The cross section of the nanodiscs is well-presented with a thickness of $\sim$20 nm. Fig. 2c and d shows the face-up TEM images for Co_3O_4 nanodiscs. The width of the nanodisc is $\sim$200 nm. We also observe that these nanodiscs exhibit a porous structure with the pore size ranging from a few nanometers to $\sim$20 nm.

Fig. 3 shows the nitrogen adsorption–desorption isotherms and the pore size distributions for Co_3O_4 nanodiscs. Using the Brunauer–Emmett–Teller (BET) method, the surface area of the Co_3O_4 hexagonal nanodiscs is measured to be 60 $m^2\ g^{-1}$. According to the

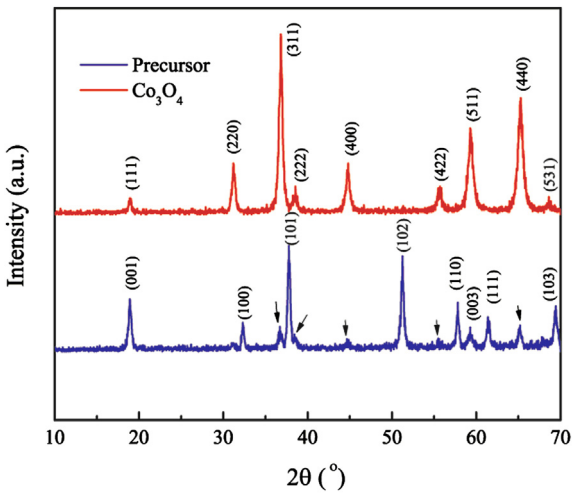

Fig. 1. XRD patterns of the precursor (a) prepared by hydrothermal method and (b) its annealed product in air at 450 °C for 2 h.

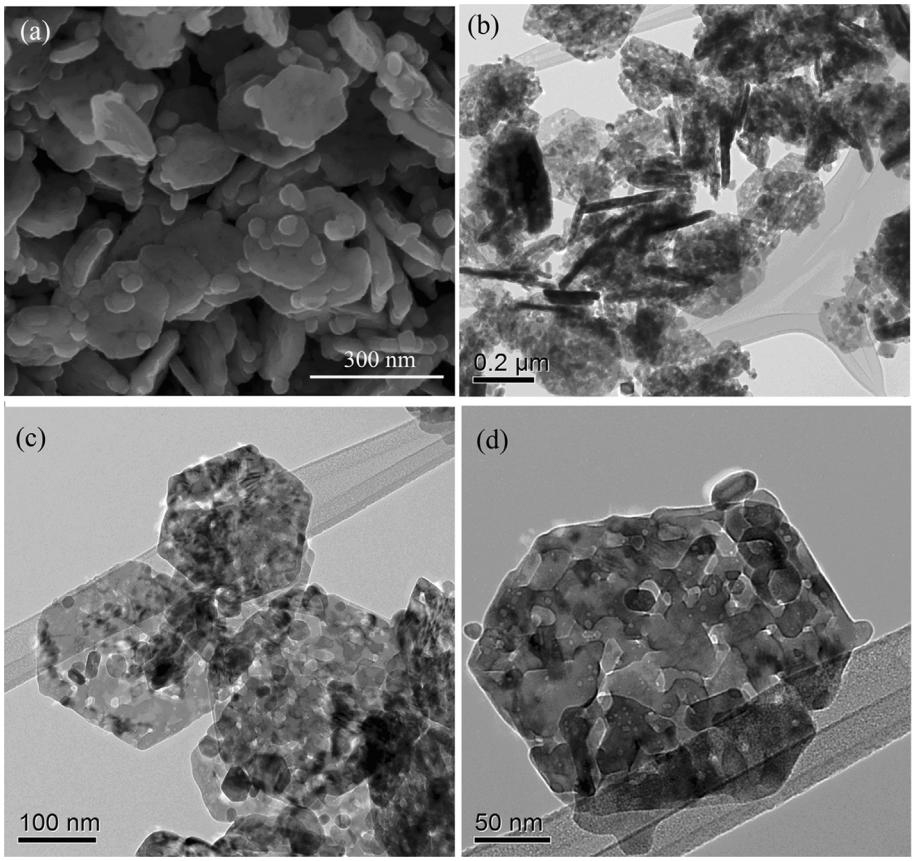

Fig. 2. SEM image (a) and TEM (b, c, d) images of Co_3O_4 nanodiscs annealed in air at 450 °C for 2 h.

pore size distribution and the isotherms, most of the pore sizes range from 2 to 30 nm. This result correlates well with TEM results indicating that most of the pores are relatively large in size. The pore volume is 0.233 $cm^3\ g^{-1}$. All of these characteristics favorably accommodate the volumetric changes that occur in electrode materials during charge/discharge cycles. Furthermore, the relative low surface area would reduce the risk of electrolyte decomposition and increase the Columbic efficiency [16].

Fig. 4 shows the cycling performance of Co_3O_4 nanodiscs when cycled between 0.01 and 3 V vs. Li/Li^+ at a current density of 100 mA g^{-1}. The initial discharge and charge capacities of the Co_3O_4 nanodiscs are of 1417 mAh g^{-1} and 1023 mAh g^{-1}, respectively, based on the total weight of Co_3O_4 and conductive carbon. This value is larger than the theoretical capacity of 890 mAh g^{-1} for Co_3O_4. The extra capacity measured in this work can be attributed to the initial solid electrode interface (SEI) structure stabilization during the formation process. Our nanodisc electrode has a much better initial Columbic efficiency (72%) when compared with that of the nanomesh electrode (~50%) [29].

The better reversibility exhibited by our porous Co_3O_4 nanodiscs can be attributed to their much lower surface area. As indicated by nitrogen adsorption–desorption measurements, the Co_3O_4 nanodiscs have a surface area of 60 $m^2\ g^{-1}$. The capacity decrease for the first cycles can be attributed to the formation of the SEI layer and the consumption of electrolytes. After 5 cycles, the capacities begin to increase steadily. The Columbic efficiency increases to 99% after 4 cycles and remains very stable. After 100 cycles, the specific discharge/charge capacities are 1180 mAh g^{-1} and 1161 mAh g^{-1}, respectively. This improvement is attributed to the activation process of the electrode materials by deeper cycling and electrochemical grinding. A similar phenomenon was observed by Xia and co-workers in hollow Co_3O_4 nanowire arrays [21]. In their report, the capacities continue to increase to 1000 cycles, at which point the capacities become quite stable. After activation, the specific capacities detected at various rates doubled. The high reversible capacity beyond the theoretical capacity can probably be attributed to the porous structures of the nanodiscs. In the nanostructured systems, lithium surface storage may play an important role in the overall capacity [32]. The pores within the nanodiscs can provide extra sites for the lithium surface storage during cycling, thus higher capacity larger than the theoretical capacity are delivered. Similar phenomenon has been reported for nanometer-sized $Li_4Ti_5O_{12}$ electrodes in activated carbon/$Li_4Ti_5O_{12}$ batteries based on nonaqueous electrolytes [33]. The specific capacities obtained in our work are three times more than the theoretical capacity of commercially used graphite (372 mAh g^{-1}) anode [13]. This result also is better than the electrochemical performance reported for pompon-like microspheres [30], which exhibit a rapid decrease in capacity after 30 cycles and deliver a specific capacity of 800 mAh g^{-1} after 50 cycles. Porous Co_3O_4 nanoneedle arrays prepared directly on copper foil [25] exhibit ultra-fast charging/discharging performance. However, only 70% percent of the first charge capacity is retained. This decrease in performance is attributed to the presence of broken nanoneedle thin tips in the electrolyte. As mentioned above, porous nanomesh electrodes show extremely high capacities at the initial cycles; however, it degrades rapidly to 800 mAh g^{-1} after 50 cycles [29]. In our case, the charge capacities continue to increase, which suggests that the two-dimensional Co_3O_4 nanodiscs are better at maintaining the integrity of the nanoparticles. Fig. 4b shows the discharging and charging curves for the 1st, 20th, 50th, and 100th cycles. In

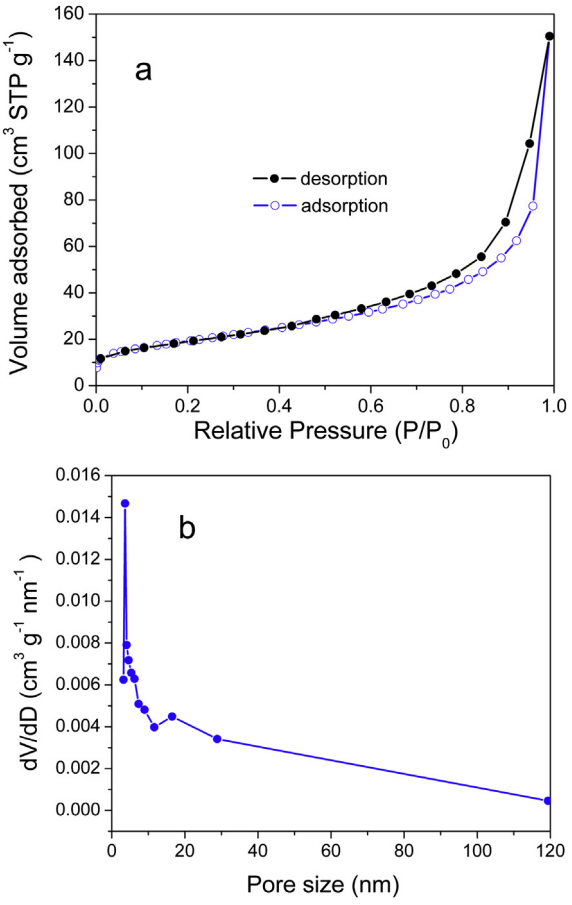

Fig. 3. Nitrogen adsorption–desorption isotherms (a) along with the corresponding pore size distributions (b) of the Co_3O_4 nanodiscs calcined at 450 °C.

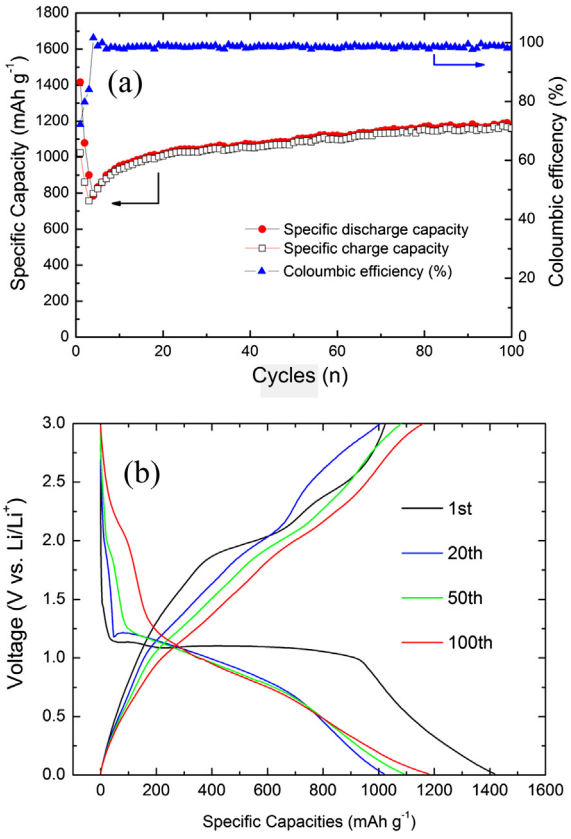

Fig. 4. The cycling performance (a) of Co_3O_4 nanodiscs and (b) the discharge/charge curves of 1st, 20th, 50th, and 100th cycles at 100 mA g^{-1} between 0.01 and 3 V vs. Li/Li^+.

the first discharge curve, two well-defined voltage plateaus at approximately 1.2 and 1.0 V correspond to the reduction processes to CoO and metallic cobalt [34,35]. According to Fig. 4b, it seems that the increased capacity is attributed to the increased lithiation capacity above ~1.2 V by comparison of the 20th, 50th and 100th cycles. The results can be explained by the decreased polarization of the Co_3O_4 nanodiscs electrode upon cycling. According to the TEM images, nanopores are clearly observed within the Co_3O_4 nanodiscs. It is believed that the wettability of the Co_3O_4 nanodiscs can be improved upon cycling and electrochemical grinding, thus lower polarization can be achieved.

Fig. 5 shows the rate capability of Co_3O_4 nanodiscs between 0.01 and 3 V vs. Li/Li^+. After discharging/charging at 100 mA g^{-1} for 5 cycles, the electrode cycled at a current density of 500 mA g^{-1}. The continuous capacity increase is similar to the phenomenon shown in Fig. 4. The improved wettability of the electrolyte–solid electrode interphase and the activation of the electrode materials by cycling would be the main reasons for the capacity increase. At the 50th cycle, a specific charge capacity of 1009 mAh g^{-1} was delivered. After another 50 cycles at 1 A g^{-1}, the nanodiscs released a specific charge capacity of 926 mAh g^{-1}. The electrodes then were discharged/charged for 50 cycles at a current density of 2 A g^{-1}, 4 A g^{-1}, and 8 A g^{-1} and demonstrated a specific charge capacity of 800 mAh g^{-1}, 560 mAh g^{-1}, and 347 mAh g^{-1}, respectively. After 250 cycles, the current density decreased to 500 mA g^{-1}. It exhibits an extremely high specific charge capacity of 1086 mAh g^{-1}, nearly 100% Columbic efficiency, and good cycle stability. To the best of our knowledge, this performance is among the best ever reported for a cobalt-based anode. These results demonstrate that porous hexagonal nanodiscs show promise as anode materials for lithium-ion batteries. The excellent rate capability and cycle stability are attributed to following factors: (1) the high purity and the relatively small surface area decrease the risk of electrolyte decomposition; (2) the nano-sized thickness (~20 nm) of the hexagonal nanodiscs reduces the lithium ions diffusion and electron-transportation distances; (3) the porous structures within the hexagonal nanodiscs facilitate the electrolyte penetration and provide extra sites for lithium surface storage.

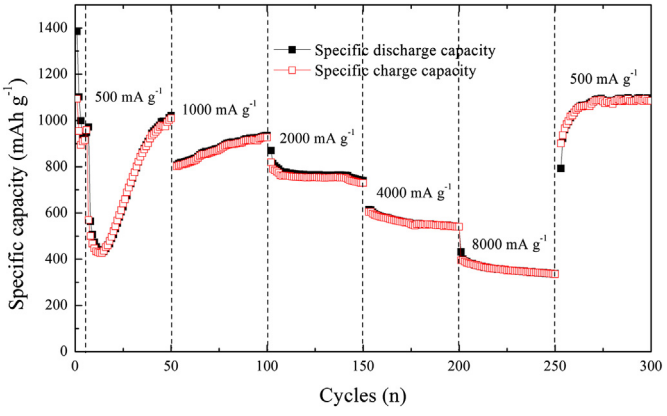

Fig. 5. Rate performance of Co_3O_4 nanodiscs vs. cycles in the voltage range of 0.01–3 V vs. Li/Li^+.

4. Conclusions

In summary, we have successfully fabricated Co_3O_4 hexagonal nanodiscs by annealing a hydrothermally prepared $Co(OH)_2$ precursor (without using any surfactant) in air at 450 °C for 2 h. The as-synthesized Co_3O_4 porous nanodiscs are ~20-nm thick, and the surface area is 39 $m^2\ g^{-1}$. The pore size of the porous Co_3O_4 ranges from a few nanometers to 20 nm. The Co_3O_4 nanodiscs exhibit a specific charge capacity of 1161 mAh g^{-1} after 100 cycles at a current density of 100 mA g^{-1} and good reversibility. It delivers specific charge capacities of 1009, 926, 800, 560, and 347 mA h g^{-1} at current densities of 0.5, 1, 2, 4, and 8 A g^{-1}, respectively. These results demonstrate that porous Co_3O_4 nanodiscs synthesized using our template-free method are promising anode materials for lithium-ion batteries.

Acknowledgments

We acknowledge the financial support provided by the National Nature Science Foundation of China (No. 51302323), the Lie-Ying Program of Central South University, the Laboratory Directed Research and Development Program at Pacific Northwest National Laboratory (PNNL), and the Batteries for Advanced Transportation Technologies Program (BATT) of the U.S. Department of Energy's (DOE) Office of Vehicle Technology. The SEM and TEM measurements were performed at the Environmental Molecular Sciences Laboratory, a national scientific-user facility sponsored by DOE's Office of Biological and Environmental Research. DOE's Office of Basic Energy Sciences, Division of Materials Sciences and Engineering, also provided support under Award KC020105-FWP12152.

References

[1] C. Liu, F. Li, L.-P. Ma, H.-M. Cheng, Adv. Mater. 22 (2010) E28.
[2] N.A. Kaskhedikar, J. Maier, Adv. Mater. 21 (2009) 2664.
[3] J. Hassoun, S. Panero, P. Simon, P.L. Taberna, B. Scrosati, Adv. Mater. 19 (2007) 1632.
[4] J. Hassoun, G. Derrien, S. Panero, B. Scrosati, Adv. Mater. 20 (2008) 3169.
[5] L.-F. Cui, Y. Yang, C.-M. Hsu, Y. Cui, Nano Lett. 9 (2009) 3370.
[6] J.O. Besenhard, J. Yang, M. Winter, J. Power Sources 68 (1997) 87.
[7] Y.S. Hu, L. Kienle, Y.G. Guo, J. Maier, Adv. Mater. 18 (2006) 1421.
[8] Y. Yu, C.-H. Chen, Y. Shi, Adv. Mater. 19 (2007) 993.
[9] W.-Y. Li, L.-N. Xu, J. Chen, Adv. Mater. 15 (2005) 851.
[10] P. Meduri, C. Pendyala, V. Kumar, G.U. Sumanasekera, M.K. Sunkara, Nano Lett. 9 (2009) 612.
[11] J.L.C. Rowsell, V. Pralong, L.F. Nazar, J. Am. Chem. Soc. 123 (2001) 8598.
[12] B. Li, H. Cao, J. Shao, G. Li, M. Qu, G. Yin, Inorg. Chem. 50 (2011) 1628.
[13] Z.-S. Wu, W. Ren, L. Wen, L. Gao, J. Zhao, Z. Chen, G. Zhou, F. Li, H.-M. Cheng, ACS Nano 4 (2010) 3187.
[14] Y. Wang, H.J. Zhang, L. Lu, L.P. Stubbs, C.C. Wong, J. Lin, ACS Nano 4 (2010) 4753.
[15] P.G. Bruce, B. Scrosati, J.M. Tarascon, Angew. Chem. Int. Ed. 47 (2008) 2930.
[16] H. Li, Z.X. Wang, L.Q. Chen, X.J. Huang, Adv. Mater. 21 (2009) 4593.
[17] J.S. Chen, T. Zhu, Q.H. Hu, J.J. Gao, F. Su, S.Z. Qiao, X.W. Lou, Appl. Mater. Interfaces 2 (2010) 3628.
[18] T. He, D.R. Chen, X.L. Jiao, Y.L. Wang, Y.Z. Duan, Chem. Mater. 17 (2005) 4023.
[19] Y.G. Li, B. Tan, Y.Y. Wu, Nano Lett. 8 (2008) 265.
[20] K.M. Shaju, F. Jiao, A. Debart, P.G. Bruce, Phys. Chem. Chem. Phys. 9 (2007) 1837.
[21] X.-H. Xia, J.-P. Tu, Y.-J. Mai, X.-L. Wang, C.-D. Gu, X.-B. Zhao, J. Mater. Chem. 21 (2011) 9319.
[22] X. Xie, Y. Li, Z.-Q. Liu, M. Haruta, W. Shen, Nature 458 (2009) 746.
[23] X.W. Lou, D. Deng, J.Y. Lee, L.A. Archer, J. Mater. Chem. 18 (2008) 4397.
[24] N. Du, H. Zhang, B. Chen, J. Wu, X. Ma, Z. Liu, Y. Zhang, D. Yang, X. Huang, J. Tu, Adv. Mater. 19 (2007) 4505.
[25] X.-Y. Xue, S. Yuan, L.-L. Xing, Z.-H. Chen, B. He, Y.-J. Chen, Chem. Commun. 47 (2011) 4718.
[26] Y.L. Hou, H. Kondoh, M. Shimojo, T. kogure, T. Ohta, J. Phys. Chem. B 109 (2005) 19094.
[27] Z.P. Liu, R.Z. Ma, M. Osada, T. Sasaki, J. Am. Chem. Soc. 127 (2005) 13869.
[28] J.T. Sampanthar, H.C. Zeng, J. Am. Chem. Soc. 124 (2002) 6669.
[29] Y. Wang, H.J. Zhang, J. Wei, C.C. Wong, J. Lin, A. Borgna, Energy Environ. Sci. 4 (2011) 1845.
[30] B. Guo, C. Li, Z.-Y. Yuan, J. Phys. Chem. C 114 (2010) 12805.
[31] H.-W. Shim, Y.-H. Jin, S.-D. Seo, S.-H. Lee, D.-W. Kim, ACS Nano 5 (2011) 443.
[32] Y.G. Guo, J.S. Hu, L.J. Wan, Adv. Mater. 20 (2008) 2878.
[33] G.G. Amatucci, F. Badway, A.D. Pasquier, T. Zheng, J. Electrochem. Soc. 148 (2001) A930.
[34] X.W. Lou, D. Deng, J.Y. Lee, J. Feng, L.A. Archer, Adv. Mater. 20 (2008) 258.
[35] J. Liu, H. Xia, L. Lu, D.F. Xue, J. Mater. Chem. 20 (2010) 1506.